2. Materials and Methods

2.1 Chemicals and Biochemicals

For the ATPase measurement, the following compounds and therapeutic drugs were purchased from commercial sources indicated in parentheses: epinephrine, norepinephrine, γ-aminobutyric acid, serotonin, melatonin, nifedipine, bepridil, fendiline, prenylamine, nicardipine, dexamethasone, prednisolone, cortisone, pinacidil, acetylsalicylic acid, indomethacin, acemetacin, ibuprofen, naproxen, mepirizole, vinblastine, etoposide, doxorubicin, daunorubicin, paclitaxel, 5-fluorouracil, quinidine, *p*-aminohippuric acid, penicillin G, novobiocin, malachite green, and polyvinyl alcohol (Sigma-Aldrich Japan KK, Tokyo, Japan); glutamic acid, dopamine, histamine, verapamil, diltiazem, betamethasone, nicorandil, actinomycin D, and methotrexate (Wako Pure Chemical Industries, Ltd., Osaka, Japan); glycine, ATP magnesium salt, Tris, Mes, EGTA, dithiothreitol, ouabain, and trichloroacetic acid (Nacalai Tesque, Inc., Kyoto, Japan); FK506 (Calbiochem, Darmstadt, Germany). All other chemicals were of analytical grade. The human P-glycoprotein expressed in Sf9 cell membranes, as the positive control, was purchased from GENTEST/BD Biosciences (Woburn, MA, USA).

2.2 Expression of ABCB1 in Sf9 insect cells

Human ABCB1 was expressed in insect *Spodoptera frugiperda* Sf9 cells using the pFASTBAC1 vector (Figure 1A), where the ABCB1 cDNA was inserted between the *Sac*I and *Xho* I restriction enzyme sites. Recombinant baculoviruses encoding the ABCB1 cDNA were generated with the BAC-TO-BAC Baculovirus Expression Systems (Invitrogen) according to the manufacturer's instructions. Sf9 cells (1×10^6 cell/ml) were then infected with the recombinant baculoviruses and cultured in EX-CELL™ 420 Insect serum-free medium (JRH Bioscience, Levexa, KS, USA) at 26°C with gentle shaking. The expression of ABCB1 in Sf9 cells increased during the incubation (Figure 1B). Three to 4 days after the infection, cells were harvested by centrifugation. Cells were subsequently washed with phosphate-buffered saline (PBS) at 4°C, collectied by centrifugation, and stored at –30°C until used.

2.3 Preparation of the plasma membrane from Sf9 cells

The cell pellet was thawed quickly and diluted 40-fold with a hypotonic buffer (0.5 mM Tris/Hepes, pH 7.4. and 0.1 mM EGTA) and then homogenized with a Potter-Elvehjem homogenizer. After centrifugation at 9,100 x *g*, the supernatant was further centrifuged at 100,000 x *g* for 30 min. The resulting pellet was suspended in 250 mM sucrose containing 10 mM Tris/Hepes, pH 7.4. The crude membrane fraction was layered over 40% (w/v) sucrose solution and centrifuged at 100,000 x *g* for 30 min. The turbid layer at the interface was collected, suspended in 250 mM sucrose containing 10 mM Tris/Hepes, pH 7.4, and centrifuged at 100,000 x *g* for 30 min. The membrane fraction was collected and resuspended in a small volume (150 to 250 μl) of 250 mM sucrose containing 10 mM Tris/Hepes, pH 7.4. After the measurement of protein concentration by the BCA Protein Assay Kit (PIERCE, Rockford, IL, USA), the membrane solution was stored at –80 °C until used.

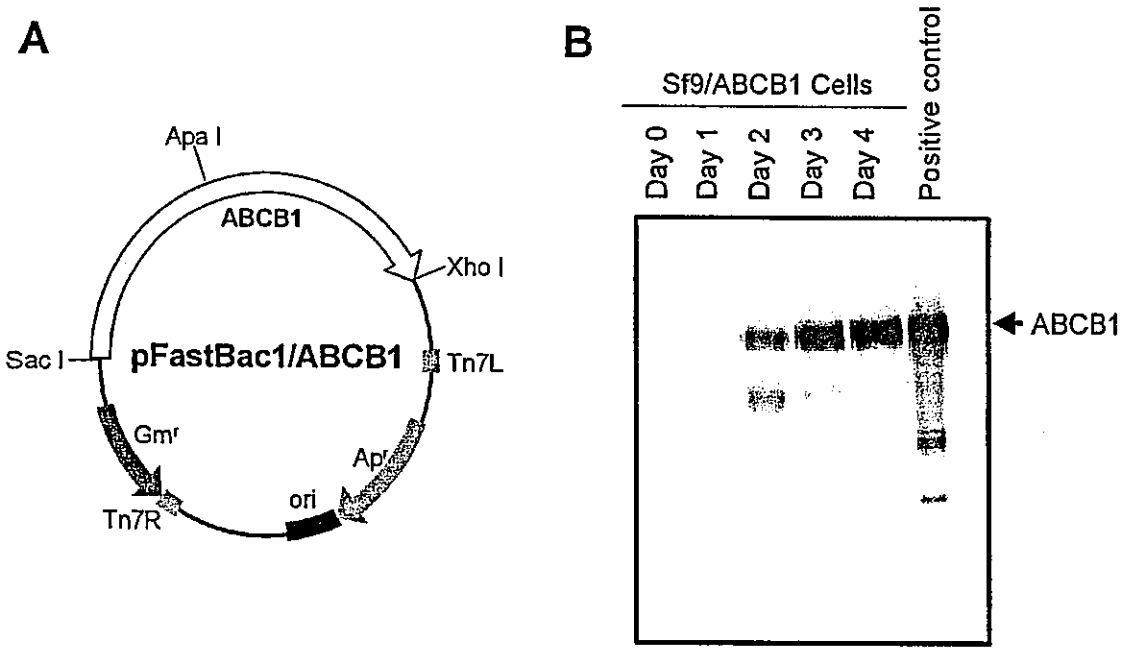

Figure 1. Expression of ABCB1 in Sf9 cells.
A, pFASTBAC1 vector encoding the cDNA of human ABCB1 (P-glycoprotein). B, Expression levels of ABCB1 in Sf9 cell membrane. The plasma membrane was prepared from Sf9 cells after infection with recombinant baculoviruses on the days indicated. ABCB1 protein was detected by western blot as described in Materials and Methods.

2.4 Immunological detection of ABCB1 expression in plasma membrane

The ABCB1 protein expressed in Sf9 cell membranes were detected by the western blot method using the C219 monoclonal antibody (SIGNET, Dedham, MA, USA). Briefly, proteins of the isolated plasma membrane were separated by electrophoresis on 7.5% sodium dodecyl sulfate (SDS) polyacrylamide slab gels and electroblotted onto Hy-bond ECL nitrocellulose membranes (Amersham, Buckinghamshire, UK). Immunoblotting was performed by using the C219 monoclonal antibody (1:250 dilution) as the first antibody and an anti-mouse IgG-horseradish peroxidase (HRP)-conjugate (Cell Signaling Technology, Beverly, MA, USA)(1:3000 dilution) as the secondary antibody. HRP-dependent luminescence was developed by using Western Lighting Chemiluminescent Reagent Plus (PerkinElmer Life Sciences, Boston, MA, USA) and detected by Lumino Imaging Analyzer FAS-1000 (TOYOBO, Osaka, Japan).

2.5 Measurement of ABCB1 ATPase activity with a high-speed screening system

The ATPase activity of the isolated Sf9 cell membranes was determined by measuring inorganic phosphate liberation [9] according to the procedure reported by Sarkadi et al. [10] with some modifications. In the present study, we have developed a high-speed screening protocol using 96-well plates (Figure 2). Briefly, the Sf9 cell membranes (2 μg of protein per each well) were suspended in 10 μl of the incubation medium containing 50 mM Tris-Mes (pH 6.8), 2mM EGTA, 2 mM ouabain, 2 mM dithiothreitol, 50 mM potassium chloride, and 5 mM sodium azide.

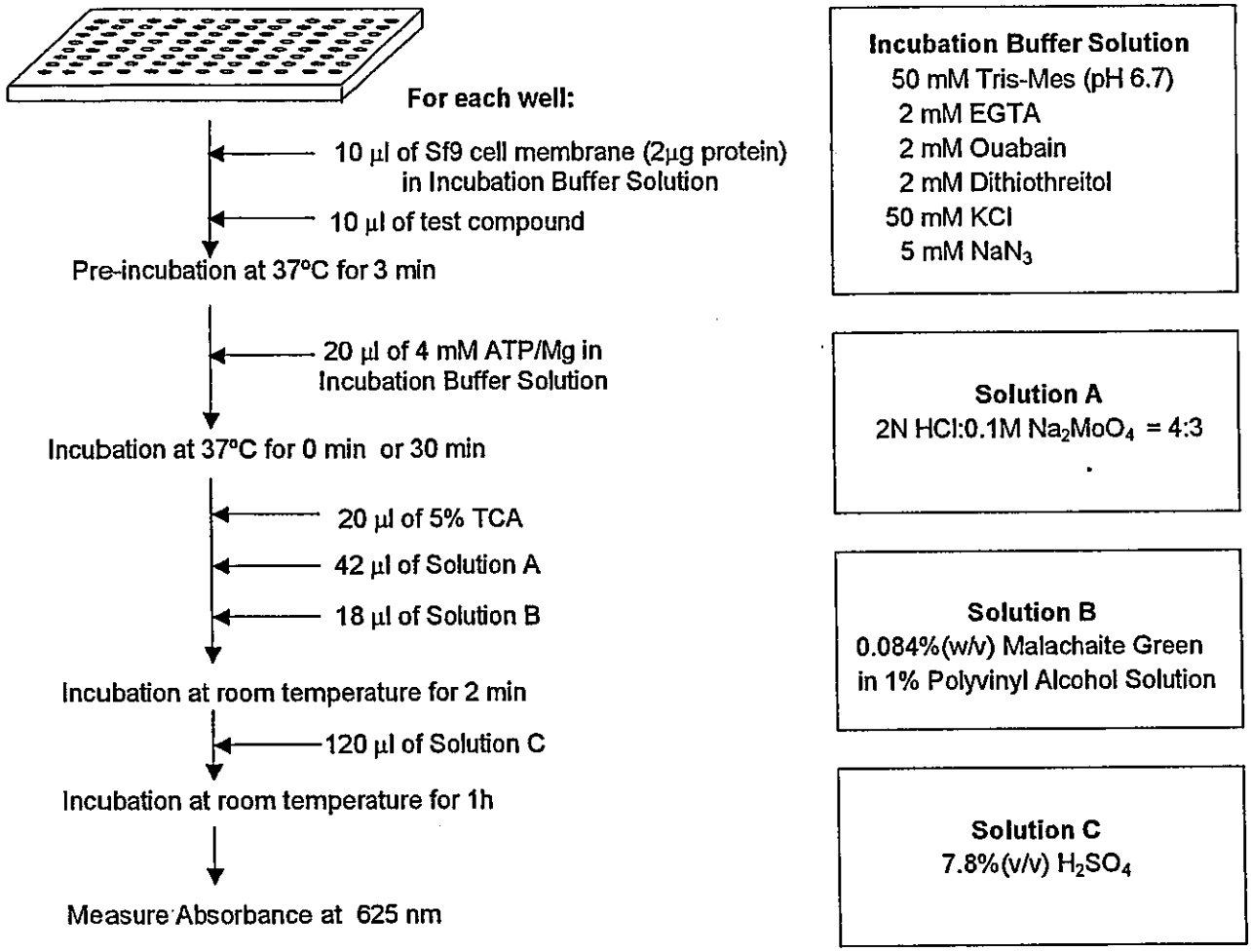

Figure 2. Schematic diagram for the high-speed screening of ABCB1 ATPase activity.

This medium was mixed with 10 μl of a test compound solution and then pre-incubated at 37°C for 3 min. The ATPase reaction was started by adding 20 μl of 4 mM ATP solution to the reaction mixture, and the incubation was maintained at 37°C for 30 min or stopped immediately. After the incubation, the reaction mixture was mixed with 20 μl of 5% trichloroacetic acid and subsequently with 42 μl of "solution A" and "solution B" (see Figure 2 for details). Thereafter, 120 μl of "solution C" was added to the mixture (Figure 2). These mixing processes were automatically carried out in the HALCS-I system (BioTec Co. Ltd., Tokyo Japan) (Figure 3A). The absorbance of each reaction mixture in the 96-well plates was photometrically measured at a wavelength of 625 nm in a Multiskan JX system (Dainippon Pharmaceuticals Co., Osaka, Japan) (Figure 3B). The amount of liberated phosphate was quantified based on the calibration line established with inorganic phosphate standards (Figure 3C). In addition, each 96-well plate contained a positive control, in which Sf9 cell membranes were incubated with 10 μM verapamil (Figure 3C).

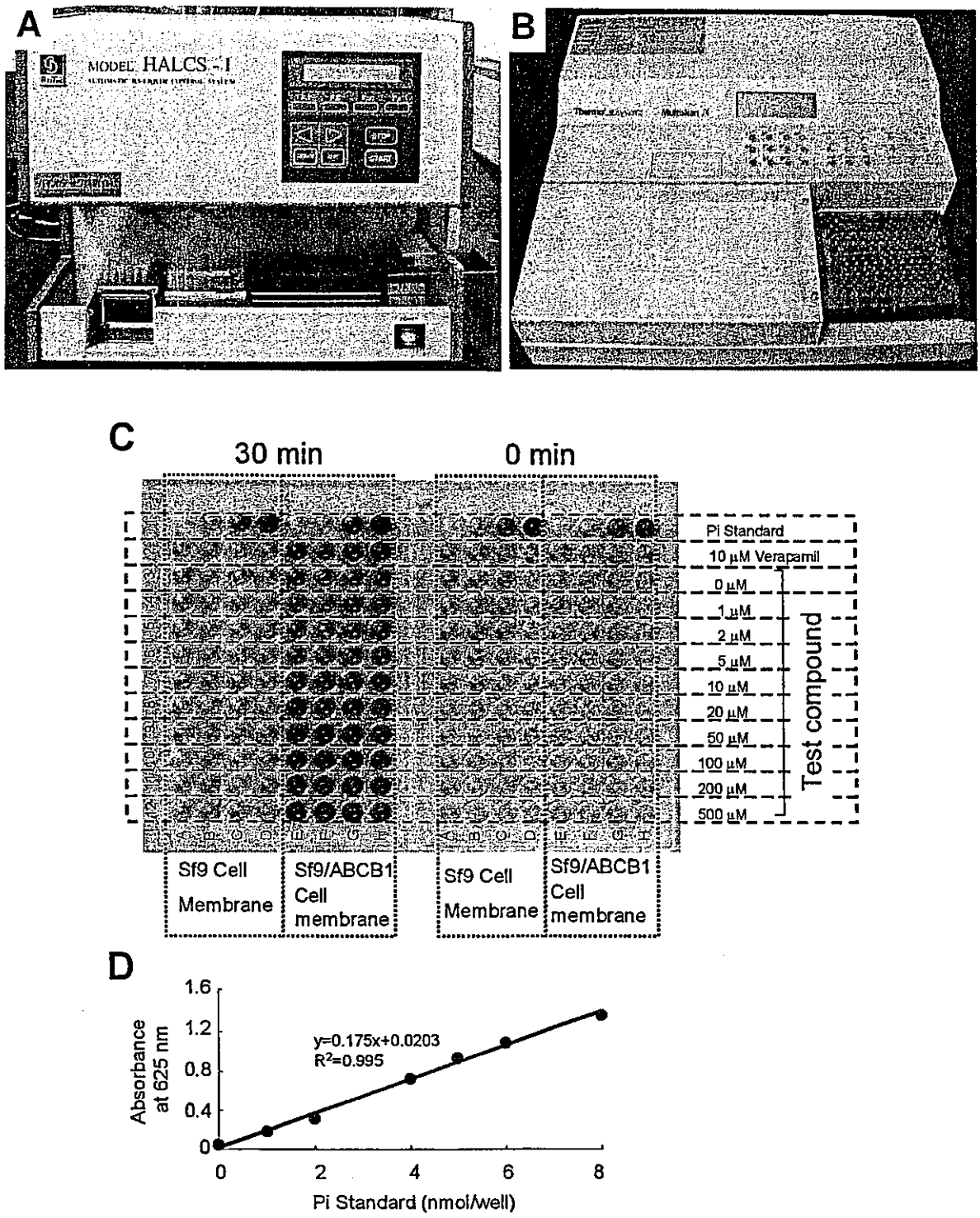

Figure 3. The high-speed screening system for the measurement of ABCB1 ATPase activity.
A, HALCS-I system (BioTec Co. Ltd., Tokyo Japan); B, Multiskan JX 96-well plate reader (Dainippon Pharmaceuticals Co., Osaka, Japan); C, an example of 96-well plates prepared for ABCB1 ATPase assay; D, relationship between the standard Pi concentration and the absorbance at 625nm.

2.6 Measurement of the surface activity

The surface activity was measured essentially according to Seelig et al. [11] and Fischer *et al.* [12] By using a Multi Pi-multi-channel microtensiometer WS/1 workstation (Kibron Inc., Helsinki, Finland). A 10-mM Tris/HCl buffer (pH 7.4) containing 154-mM NaCl was used as the solvent for all test compounds. The stock solutions were prepared by dissolving drugs in dimethyl sulfoxide (DMSO) at a concentration of 10 mM. The stock solution of each drug was injected in small increments by means of a microsyringe to achieve the desired concentrations in the above-mentioned Tirs/HCl buffer solution (10^{-6} to 10^{-3} M). The critical micelle concentration (CMC) and the air-water partition coefficient (K_{aw}) were obtained from plots of the surface tension versus the logarithm of test compound concentrations.

2.7 SAR analysis using chemical fragmentation codes

To execute the SAR analysis for the compounds and drugs tested in this study, we generated their chemical fragmentation codes by using the Markush TOPFRAG program [13] (Derwent Information, Ltd., London, UK). The chemical fragment codes are a set of alphanumeric symbols, each representing a fragment of a chemical structure. The Markush TOPFRAG program is a tool for searching the chemical structures and structure information in Derwent's online databases [14]. In the present study, we have formulated the ABCB1 ATPase activity as a linear combination of chemical fragmentation codes, each of which was weighted by the corresponding coefficient as follows:

$$\text{ABCB1 ATPase activity (Predicted)} = \Sigma\, C(i) \times \text{Chem. Frag. Code } (i) + \text{Constant}$$

The symbol of "*i*" in the parentheses designates a specific chemical fragmentation code. Based on the chemical fragmentation codes thus obtained and in comparison with the observed ATPase activity for each test compound, we have calculated chemical fragmentation coefficients, C(*i*), by multiple linear regression analysis.

3. Results

3.1 Characterization of verapamil-stimulated ABCB1 ATPase activity

In the present study using our high-speed screening system, we have investigated the substrate specificity of ABCB1 towards a variety of drugs and compounds. A plasma membrane fraction of Sf9 insect cells overexpressing human ABCB1 was used to measure the ATPase activity. As demonstrated in Figure 4, verapamil, one of the typical substrates of ABCB1, stimulated ATPase activity in the plasma membrane prepared from ABCB1-expressing Sf9 cells. The stimulation of ATPase activity was dependent on verapamil concentration, exhibiting saturation kinetics. Based on the Lineweaver-Burk plot of this result, the apparent Km value for verapamil was estimated to be 2.1 μM (data not shown). On the other hand, such stimulation of ATPase was not observed in the plasma membrane prepared from the control Sf9 cells (Figure 4). These results suggest that both the high-speed screening system and ABCB1-expressing Sf9 cell membrane are practically useful tools to evaluate the substrate specificity of ABCB1.

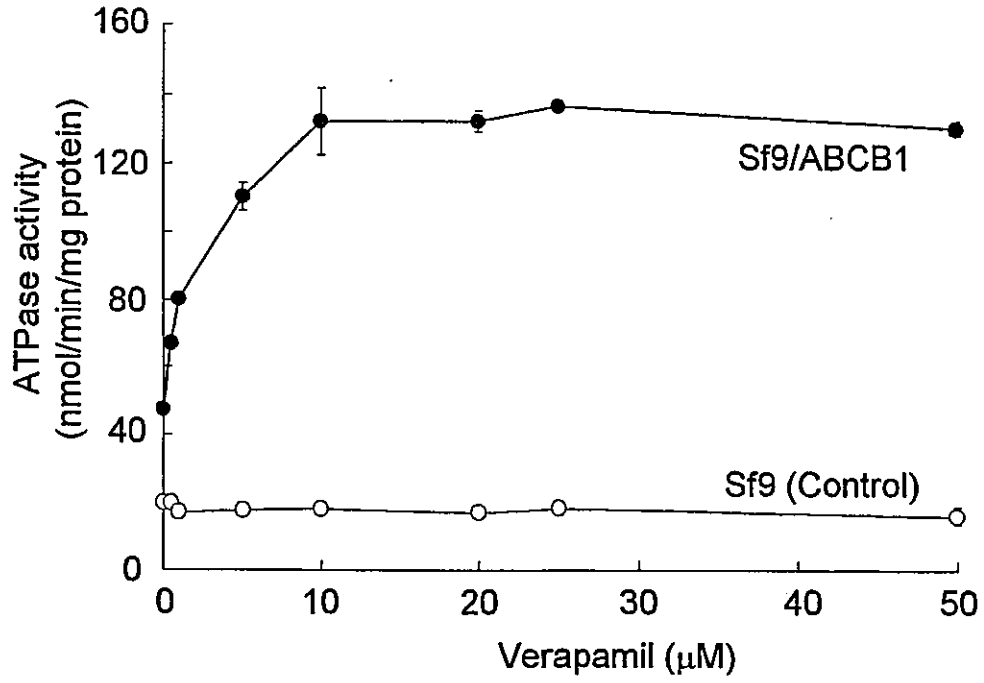

Figure 4. Effect of the verapamil concentration on the ATPase activity in the plasma membrane samples prepared from Sf9 control cells (●) or ABCB1-expressing Sf9 cells (○).
The ATPase activity was measured as described in Materials and Methods.

3.2 Effect of therapeutic drugs on ABCB1 ATPase activity

We have measured ABCB1 ATPase activity toward a total of 41 different therapeutic drugs and compounds. Figure 5 shows the molecular structures of those tested compounds. They are classified into seven groups, *i.e.*, A, neurotransmitters; B, Ca^{2+} channel blockers, C, steroids; D, potassium channel modulators; D, non-steroidal anti-inflammatory drugs (NSAIDs); F, anti-cancer drugs; and G, miscellaneous.

Figure 6 summarizes the effects of those test compounds on ABCB1 ATPase activity. The concentration of test compounds was 10 μM in the measurement, and the data are expressed as relative values as compared with the ATPase activity measured with 10 μM verapamil. Among 41 different therapeutic drugs and compounds tested in this study, Ca^{2+} channel blockers, such as verapamil (B-1), bepridil (B-4), fendiline (B-5), prenylamine (B-6), nicardipine (B-7), and FK506 (G-4) stimulated the ATPase activity. At the concentration of 100 μM, paclitaxel (F-5), doxorubicin (F-7), and quinidine (G-1) have more significantly stimulated the ABCB1 ATPase activity, whereas the extent of ATPase stimulation was relatively smaller than that of Ca^{2+} channel blockers (data not shown).

Group A

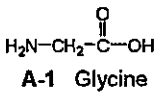

A-1 Glycine

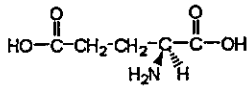

A-2 Glutamic acid

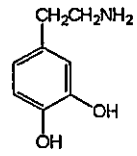

A-3 Dopamine

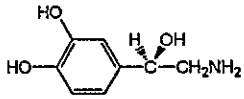

A-4 Norepinephrine

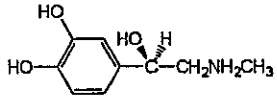

A-5 Epinephrine

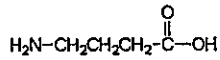

A-6 γ-Aminobutyric acid (GABA)

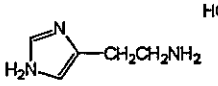

A-7 Histamine

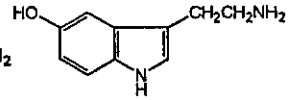

A-8 Serotonin

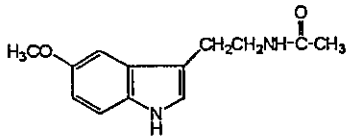

A-9 Melatonin

Group B

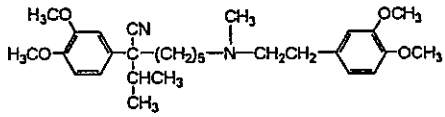

B-1 Verapamil

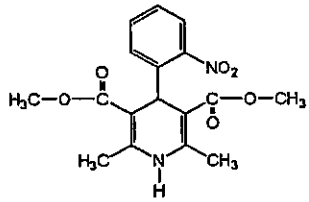

B-2 Nifedipine

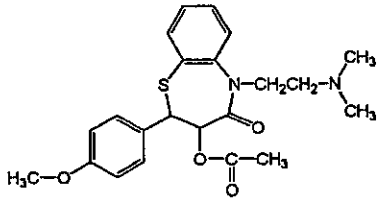

B-3 Diltiazem

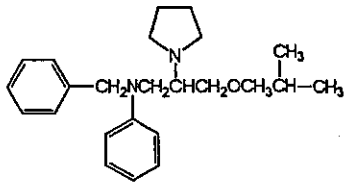

B-4 Bepridil

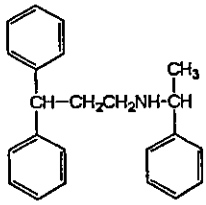

B-5 Fendiline

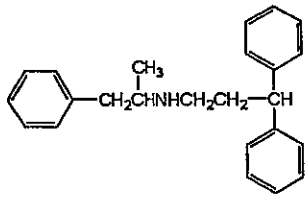

B-6 Prenylamine

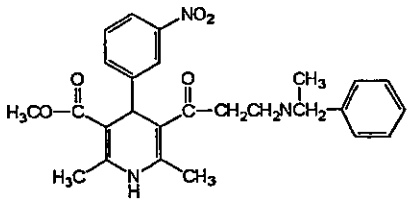

B-7 Nicardipine

Group C

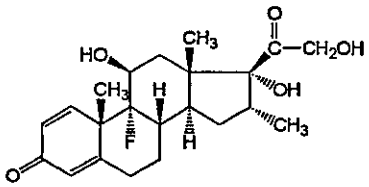

C-1 Dexamethasone

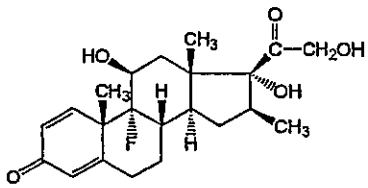

C-2 Betamethasone

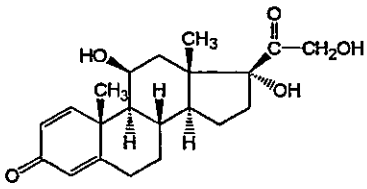

C-3 Prednisolone

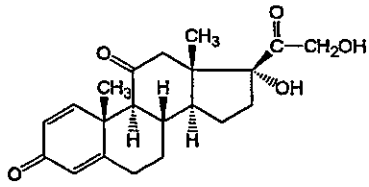

C-4 Cortisone

Group D

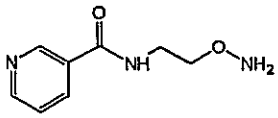

D-1 Nicorandil

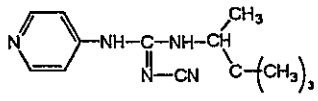

D-2 Pinacidil

Group E

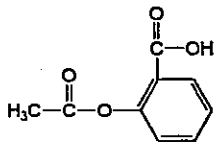

E-1 Acetylsalicylic acid

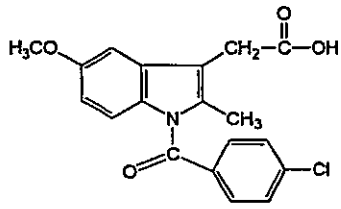

E-2 Indomethacin

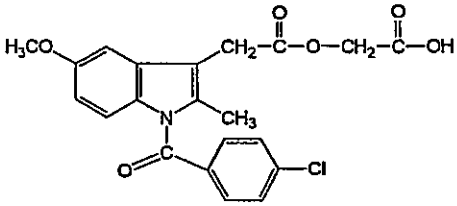

E-3 Acemetacin

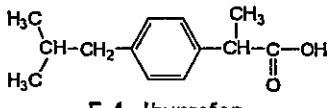

E-4 Ibuprofen

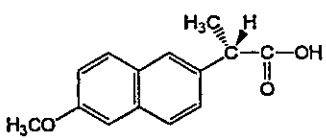

E-5 Naproxen

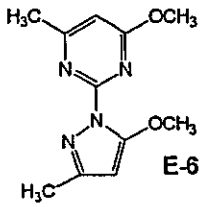

E-6 Mepirizole

Group F

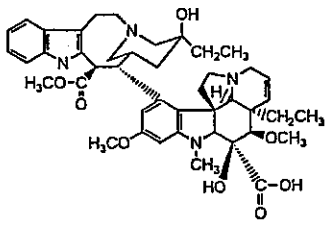

F-1 Vinblastine

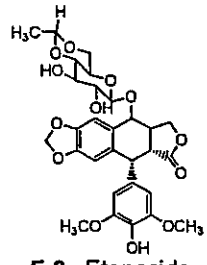

F-2 Etoposide

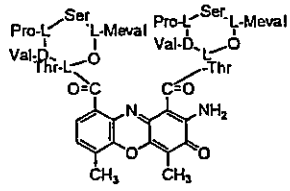

F-3 Actinomycin D

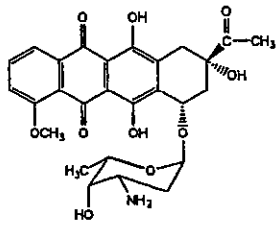

F-4 Daunorubicin

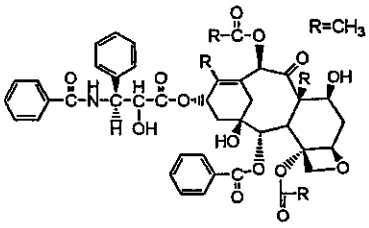

F-5 Paclitaxel

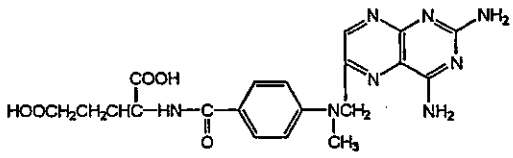

F-6 Methotrexate

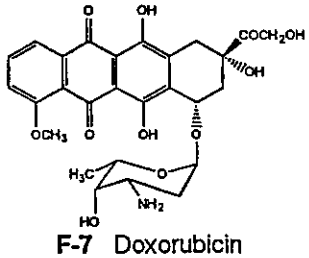

F-7 Doxorubicin

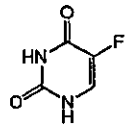

F-8 5-Fluorouracil

Group G

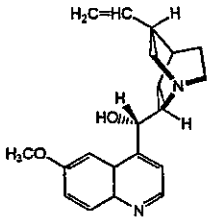

G-1 Quinidine

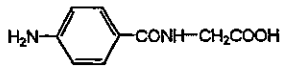

G-2 *p*-Aminohippuric acid

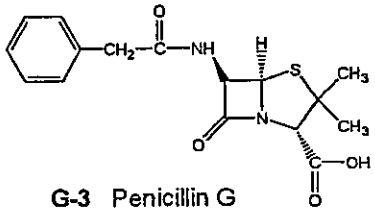

G-3 Penicillin G

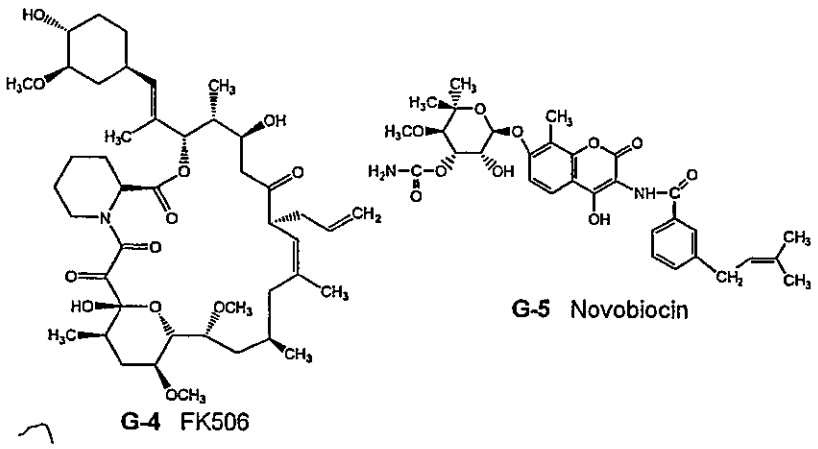

Figure 5. Molecular structures of therapeutic drugs tested for the measurement of ABCB1 ATPase activity. A, neurotransmitters; B, Ca^{2+} channel blockers, C, steroids; D, potassium channel modulators; E, non-steroidal anti-inflammatory drugs (NSAIDs); F, anti-cancer drugs; G, miscellaneous.

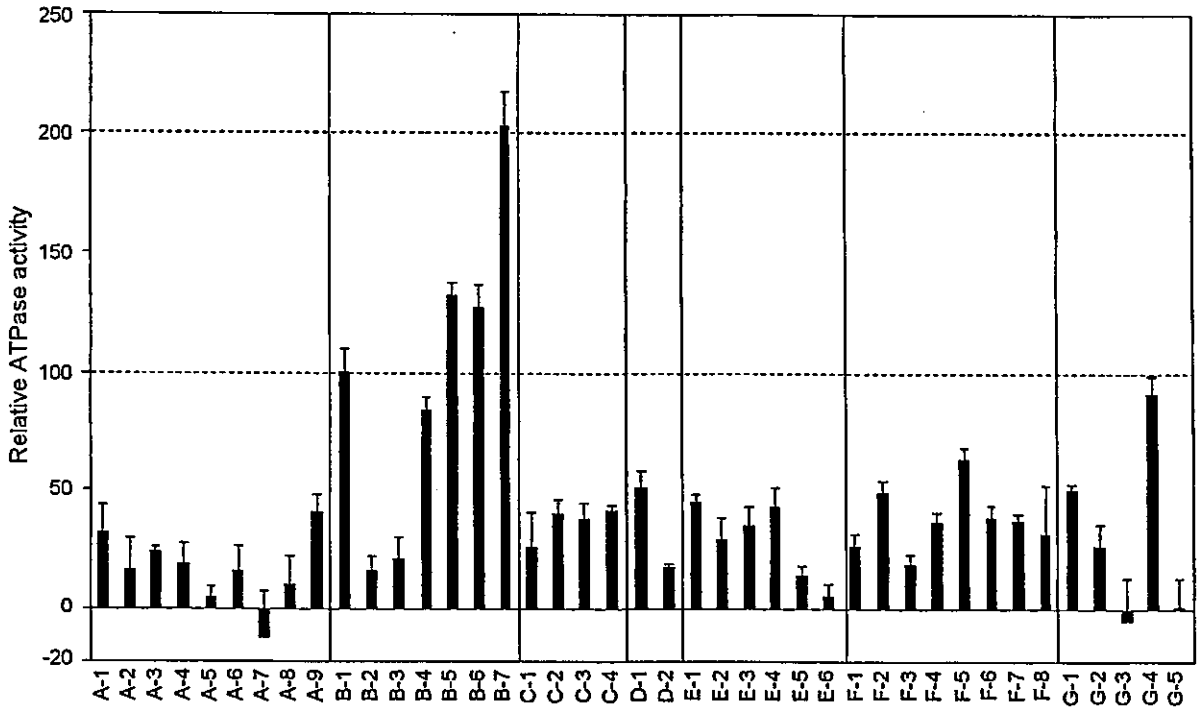

Figure 6. The effect of therapeutic drugs and compounds on ABCB1 ATPase activity.
The ATPase activity was measured in the presence of 10 μM of a test compound as described in Materials and Methods. All the activities are expressed as relative values ± S.D. as compared with the activity measured with 10 μM verapamil (100%).

3.3 Correlation of the substrate specificity of ABCB1 and the surface activity of test compounds

We have measured the surface activity of those 41 different compounds. Figure 7 demonstrates the relationship between the ABCB1 ATPase activities and the K_{aw} values of the therapeutic drugs and compounds tested. The ABCB1 ATPase activities are the same as the results presented in Figure 6. The two-dimensional plot of $\log K_{aw}$ values vs. ABCB1 ATPase activities (Figure 7) revealed that test compounds could be clearly divided into two groups, namely, ABCB1 substrate and non-substrate groups that are indicated by circles in the figure ABCB1 substrates were found to have $\log K_{aw}$ values higher than 4.3. These results suggest that ABCB1 substrates are surface-active and can be readily dissolved in the lipid bi-layer of cellular membranes.

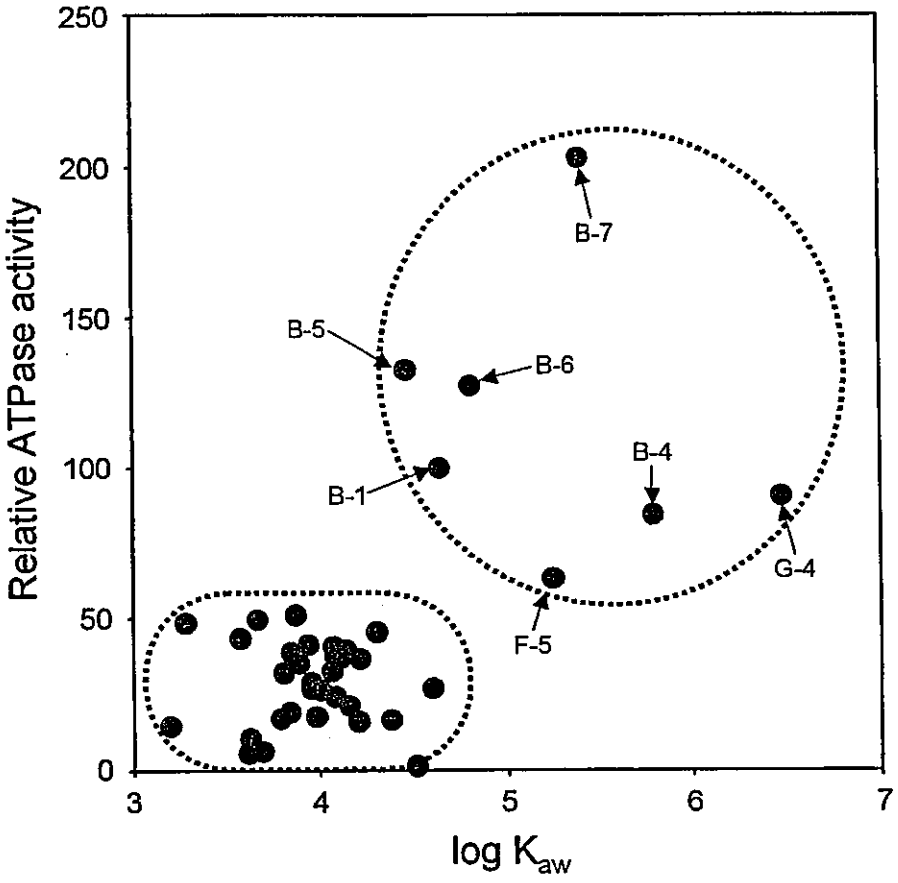

Figure 7. Relationship between the ABCB1 ATPase activities and the K_{aw} values of the therapeutic drugs and compounds tested.
The ATPase activities are expressed as relative values as compared with the activity measured with 10 μM verapamil (100%).

3.4 SAR analysis for the substrates of ABCB1

To gain more insight into the relationship between the molecular structure of compounds and the ABCB1 ATPase activity, we have performed an SAR analysis by introducing chemical fragmentation codes. The program Markush TOPFRAG was used to generate the chemical fragmentation codes based on the structures of the drugs tested. Table 1 exemplifies the chemical fragmentation codes describing the molecular structure of verapamil (B-1). In the present study, however, steroids (group C) were excluded from this analysis, because the Markush TOPFRAG program does not have an algorithm to generate chemical fragmentation codes for steroids.

Table 1. Chemical fragmentation codes describing the molecule structure of verapamil.

Verapamil
S (G100(P)H181(P)H543(P)M333(P)M414(P)M532(P)("L140" OR "L145"))/M0,M2,M3,M4
S L1(P)(M210(P)M283(P)M312(P)M316(P)M321(P)M332(P)M342(P)M343)/M2,M3,M4
S L2(P)((M370(P)M392) OR (M371(P)M373(P)M391))/M2,M3,M4
S L3(P)(M270 OR (M272(P)M273(P)M281))/M2,M3,M4
S L4(P)(G015(P)G019(P)H103(P)M211)/M2,M3,M4
S (L1(P)M900/M0) OR (L1(P)M901/M2,M3,M4) OR (L4(P)M902/M2,M3,M4)
S L6 OR L5
S L7(NOTP)(H2 OR H3 OR H4 OR H6 OR H7 OR H9 OR J0 OR J1 OR J2 OR J3)/M2,M3,M4
S L8(NOTP)(J4 OR J5 OR J6 OR J9 OR K1 OR K2 OR K3 OR K4 OR K5 OR K6)/M2,M3,M4
S L9(NOTP)(K7 OR K8 OR K9 OR "L2" OR "L3" OR "L4" OR "L5" OR "L6" OR "L7")/M2,M3,M4
S L10(NOTP)("L8" OR "L9" OR M1)/M2,M3,M4

The chemical fragmentation codes were generated by using the Markush TOPFRAG program [13] as described in Materials and Methods.

The multiple linear regression analysis delineated a clear relationship between the ABCB1 ATPase activity and chemical fragmentation codes. A total of six best-fitting models were created (Figure 8), where the predicted activity of the ABCB1 ATPase was well correlated with the observed ATPase activity. Table 2 summarizes the contents of those multiple linear regression analysis models, and Table 3 provides explanations for chemical fragmentation codes generated in the analysis. These results demonstrate that the moieties represented by the chemical fragmentation codes of J581, G100, and M331 positively contributed to the ATPase activity, whereas those of M531 and F014 had negative contributions. Among those chemical fragmentation codes, J581 had the greatest contribution (Table 2), suggesting that an oxo group bonded to an aliphatic carbon (Table 3) is an important moiety for the recognition and/or transport by the ABCB1 protein.

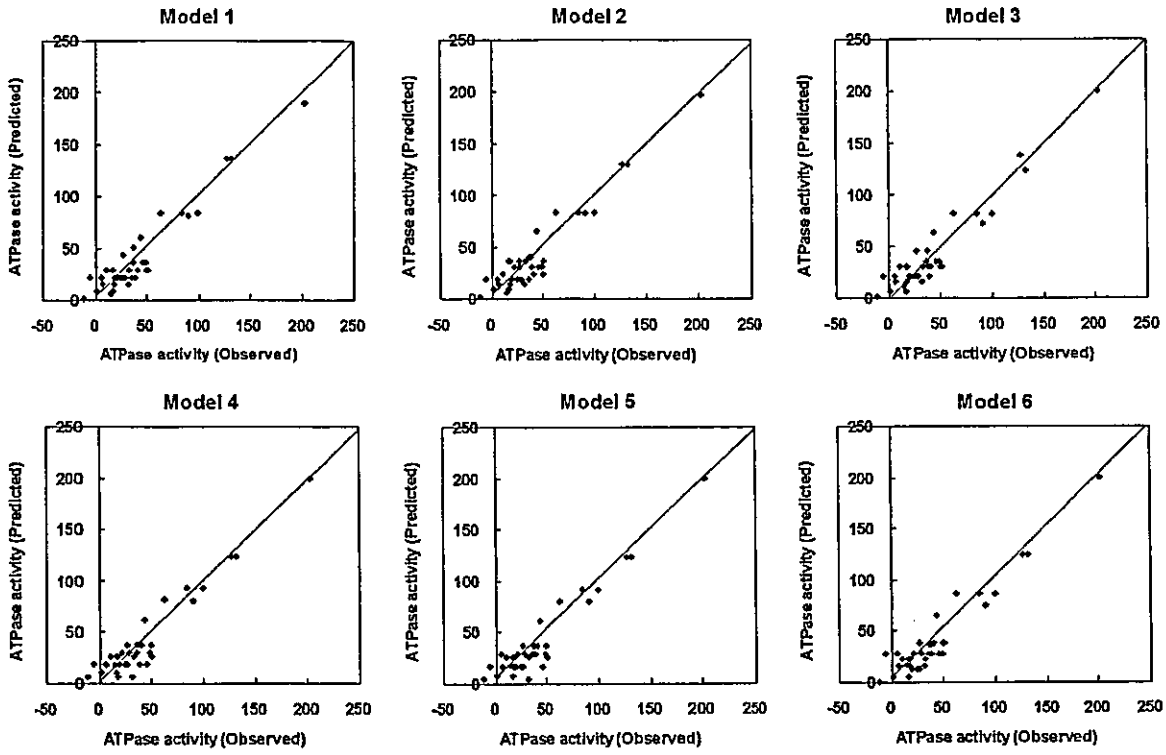

Figure 8. Relationships between the relative ATPase activity observed in Figure 6 and the activity predicted from the multiple linear regression analysis. Six models were created by the multiple linear regression analysis as demonstrated in Table 2.

Table 2. Multiple linear regression analysis models to predict ABCB1 ATPase activity toward tested compounds.

Chemical Fragmentation Code	Model 1	Model 2	Model 3	Model 4	Model 5	Model 6
J581	96.86(19.25)	90.10(22.07)	90.66(21.94)	82.85(22.49)	84.69(22.15)	97.03(22.75)
G100	54.46(12.19)	59.32(13.11)	51.62(12.46)	55.01(12.32)	54.80(12.29)	49.16(12.80)
M331	38.42(14.49)	46.44(14.37)	42.30(13.96)	42.90(14.04)	43.67(14.02)	37.71(14.46)
M270	0	0	0	0	11.61(10.53)	0
M272	0	0	0	11.40(10.47)	0	0
M531	-61.62(12.00)	-64.51(12.46)	-61.04(12.04)	-62.63(12.18)	-63.38(12.23)	-59.42(11.99)
F014	-28.32(16.03)	-22.44(14.29)	-29.08(16.49)	-19.80(13.89)	-20.93(13.98)	-22.41(13.92)
H100	0	0	0	0	0	-15.64(12.70)
M321	0	0	-14.59(12.76)	0	0	0
M370	0	-12.56(11.57)	0	0	0	0
M391	-14.29(12.29)	0	0	0	0	0
Constant	43.44(13.75)	36.61(10.31)	45.01(14.97)	26.99(9.94)	26.40(10.13)	38.79(10.77)
R =	0.953	0.952	0.953	0.952	0.952	0.954
s =	14.38	14.53	14.42	14.53	14.50	14.24
F =	47.85	46.78	47.58	46.81	47.01	48.90

The ABCB1 ATPase activity is formulated as a linear combination of chemical fragmentation codes weighted by the corresponding coefficient, where the symbol of "*i*" in the parentheses designates a specific chemical fragmentation code.
ABCB1 ATPase activity (Predicted) = $\Sigma C(i)$ x Chem. Frag. Code (i) + Constant. R: correlation coefficient, s: standard deviation, F: Fisher value (level of statistical significance).

Table 3. Explanation for the chemical fragmentation codes used for the prediction of the ABCB1 ATPase activity.

Chemical Fragmentation Code		Ext. Code	Explanation
J58	Oxo group bonded to aliphatic C	J581	One oxo group bonded to aliphatic
G1	Unfused aromatic rings	G100	Unfused aromatic ring(s) present, no other carbocyclic ring systems are present
M33	Straight or branched carbon chains	M331	Straight Carbon chain with -CH3, -C=CH2, and/or -C≡CH
M27	Chain bonded to U	M270	Chain bonded to U
M27	Chain bonded to U	M272	Chain bonded to O
M53	Carbocyclic systems with at least one aromatic ring	M531	One M53 code
F01	Positions substituted	F014	Position 4 substituted
H10	Type of amine	H100	One primary amine
M32	Multipliers for Subset M31 M31:Number of C atoms in polyvalent chain	G321	One or more M31 code used once
M37	Carbon chain bonded to ring C and (U and/or C=U and/or C≡CH) but not V, C=V, C≡V	M370	Carbon chain bonded to ring C and (U and/or C=U and/or C≡CH) but not V, C=V, C≡V
M39	Multipliers for codes M350 to M383 (polyvalent carbon chain attachments)	M391	One or more of codes used once

U= C,H,O,S,Se,Te or N
V=atom other than U

4. Discussion

4.1 High-speed screening system to analyze the substrate specificity of ABCB1

Since ABCB1 is an ATP-dependent active transporter, drug transport is coupled with ATP hydrolysis. There are two ATP-binding cassettes in one molecule of the ABCB1 protein. Those ATP-binding cassettes are functionally non-identical, but essential for the transport function of ABCB1 [15][16]. ABCB1 ATPase activity is considered a functional probe for specific binding of transported drugs. It is possible to use this property to study the function and/or substrate specificity of ABCB1 [17]. In the present study, based on the ABCB1 ATPase activity, we have developed a high-speed assay system to analyze the substrate specificity of this activity. As demonstrated in Figure 6, our assay system operated efficiently to evaluate a variety of test compounds and therapeutic drugs.

At present, there are several *in vitro* methods available for the screening of drug compounds with regard to possible stimulation or inhibition of ABCB1 activity. A common method is to incubate the compound with cells that overexpress ABCB1 and then to measure the uptake in those cells after a defined interval. The same methodology can be used to study the inhibition of ABCB1-mediated transport by measuring the uptake of known substrates, such as verapamil and doxorubicin, with and without the compound in the media. Caco-2 cell monolayers are widely used in the pharmaceutical industry to assess membrane permeability and interaction with ABCB1 and other efflux transporters [18]. However, from a drug development perspective, those cellular assay methods are too costly and time-consuming. In addition, the cell density potentially involves a critical factor that makes the estimation of ABCB1-mediated transport difficult because of the para-cellular transport of test compounds. Furthermore, there are other intrinsic drug

transporters expressed in Caco-2 cells. In this context, there is a considerable demand for rapid and efficient *in vitro* assay systems and computational methods to assess the biopharmaceutical properties of test compounds.

As compared with the Caco-2 cell system, the ATPase assay system developed in the present study is simple and makes it easy to measure the ATPase activity not only for ABCB1 but also for other ABC transporters, such as ABCG2 (BCRP/MXR1/ABCP) [19]. In addition, Sf9 insect cells and recombinant baculoviruses are practical and cost-effective mesns to express ABCB1 or other ABC transporter proteins in large amounts (Figure 1B), since Sf9 cells grow much faster than mammalian cells. As a consequence, ATPase measurements with ABCB1 expressend in Sf9 cell membranes are well suited for extensive studies involving a large number of molecules to be tested. In fact, by using our systems, we have most recently investigated the effect of genetic polymorphisms of ABCB1 on both substrate specificity and activity [2].

4.2 Correlation of the substrate specificity of ABCB1 and the surface activity of test compounds

ABCB1 was originally assumed to function as a membrane pump for exporting intracellularly located substrates. However, it has recently been proposed that ABCB1 translocates a substrate from the inner leaflet side of the membrane to the outer leaflet side, thus, it functions as a flippase or membrane vacuum cleaner. This mechanism is supported by the fact that most substrates of ABCB1 are hydrophobic compounds. Based on the latter mechanism, a substrate must be first dissolved in or adsorbed on the lipid bilayer of cellular membranes before they are recognized and subsequently transported by ABCB1. Therefore, the substrate specificity of ABCB1 is related to the lipophilicity and/or amphiphilicity of compounds.

While the lipophilicity is well characterized by the octanol/water partition coefficient (logP), Seelig *et al.* have devised a new method to predict amphiphilic properties of test compounds [11]. The criteria depend on the amphiphilic properties of a test compound as reflected in its surface activity. The surface activity is quantified by the Gibbs adsorption isotherms in terms of three parameters: (i) the onset of surface activity, (ii) the critical micelle concentration, and (iii) the surface area requirement of the test compound at the air/water interface [11].

The adsorption of an amphiphile at the air/water interface lowers the surface tension of the buffer, γ_0, to a new value γ. The difference, $\pi = \gamma_0 - \gamma$ is the so-called surface pressure. The thermodynamics of the absorption process is described by the Gibbs adsorption isotherm which can be written as

$$d\gamma = -RT(N_A A_S)^{-1}\, dlnC = -RT\Gamma dlnC = -d\pi \qquad \text{Equation (1),}$$

where C is the concentration of an amphiphilic compound in bulk solution, RT is the thermal energy, N_A is the Avogadro number and A_S is the surface area of the surface-active molecule at the interface. $\Gamma = (N_A A_S)^{-1}$ denotes the surface excess concentration. At low concentrations, Γ increases linearly with C; at high concentrations, Γ reaches a limiting value Γ^*. Thus, a plot of π vs. lnC should yield a straight line as long as Γ is constant. As was evaluated from the slope:

$$\Gamma^* = (1/RT)d\pi/dlnC \qquad \text{Equation (2).}$$

Integral forms of Equation (1) can also be given. Particularly useful for our purpose is the Szyszkowski equation [20] which may be written as :

$$\pi = RT\Gamma^* ln\,(1 + K_{aw}C) \qquad \text{Equation (3),}$$

where K_{aw} is the air/water partition coefficient. By fitting Equation (3) to the measured π/C curve

by using Γ^* determined according to Equation (2), the air/water partition coefficient, K_{aw}, was evaluated. As demonstrated in Figure 7, the two-dimensional plot of the K_{aw} values vs. ABCB1 ATPase activities revealed that test compounds could be clearly divided into two groups, namely, ABCB1 substrate and non-substrate groups. Seelig and Landwojtowicz have demonstrated that the K_{aw} value is closely related to the Km values of ABCB1 substrates [21]. These experimental results strongly suggest that the K_{aw} value is a useful indicator for the prediction of ABCB1 substrates, even better than logP values [21]. Accordingly, compounds with $\log K_{aw}$ values higher than 4.3 could be regarded as candidate substrates for ABCB1.

4.3 SAR analysis by using chemical fragmentation codes

Up to now, several research groups have intensively investigated the SAR of ABCB1 substrates [22][23][24][25][26] and tried to establish theoretical calculation methods, such as MolSurf parametrization and PLS statistics [27]. In the present study, we have taken a different approach for the SAR analysis to gain insight into the substrate specificity of ABCB1. Namely, we used the chemical fragmentation codes to describe the chemical structures of a variety of substrates and non-substrates for ABCB1. Derwent Information, Ltd., developed this structure-indexing language suitable for describing chemical patents. The chemical fragmentation codes were originally created in the early 1960's in answer to the need for accessing the increasing number of chemical patents. Markush TOPFRAG is the software that generates the chemical fragment codes from chemical structure information.

As described in this paper, we have first measured ABCB1 ATPase activity toward a total of 41 different drugs and compounds by using our high-speed screening system (Figure 6). The Markush TOPFRAG was then used to generate chemical fragmentation codes for each compound tested. The multiple linear regression analysis was carried out to gain a relationship between the ABCB1 ATPase activity and the chemical fragmentation codes thus generated. Thereby we have identified several sets of chemical fragmentation codes related to the substrate specificity of ABCB1 (Table 2). The uniqueness of this approach resides in the facts that ABCB1 ATPase activity is described as a linear combination of chemical fragmentation codes and that the coefficient for each chemical fragment code reflects the extent of the contribution of a specific chemical moiety to the ATPase activity. A total of six models were created (Table 2), and all of them indicate that one oxo group bonded to an aliphatic carbon, unfused aromatic ring(s), and straight carbon chain(s) are important chemical moieties for the substrate specificity of ABCB1. In the present analysis, however, the significance of primary amine(s) was overlooked. It would be of importance to further expand this analysis with a large number of structurally diverse compounds.

4.4 Concluding Remarks

The attrition of drug candidates in preclinical and development stages is a major problem in drug design. In least thirty percent of the cases, this attrition is due to poor pharmacokinetics (e.g., limited absorption. low plasma concentration levels, high rates of clearance). In the past, pharmaceutical companies have considered such early stage attrition an inevitable cost of doing business; however, as drug development costs have rocketed upward, pharmaceutical companies have begun to seriously re-evaluate their current strategies of drug discovery and development. Due to the development of combinatorial chemistry, there is currently an emphasis on the use of high-throughput screening using *in vitro* models to characterize the pharmacokinetic properties of potential new drug candidates. In that light, we have recently proposed that a transport mechanism-based design might help to create new, pharmacokinetically advantageous drugs, and as

such it should be considered an important component of drug design strategy [28]. The present study conveys a new strategy of efficiently analyzing the relationship between the substrate specificity of ABCB1 and chemical structures. This approach is considered to be practical and useful for the molecular design of such new drugs that can penetrate the blood-brain-barrier or circumvent the multidrug resistance of human cancer.

References

[1] T. Ishikawa, In: Cooper, D.N. (ed.) *Nature Encyclopedia of the Human Genome*, Nature Publishing Group, London, **4**, 154-160 (2003).
[2] T. Ishikawa, A. Tsuji, K. Inui, Y. Sai, N. Anzai, M. Wada, H. Endou and Y. Sumino, *Pharmacogenomics*, in press (2004).
[3] P. Borst and R. Oude Elferink, *Ann. Rev. Biochem.*, **71**, 537-592 (2002).
[4] R.B. Kim, *Curr. Opin. Drug Discov. Develop.*, **3**, 94-101 (2002)
[5] V. Ling, *Cancer Chemother. Pharmacol.*, **40**, S3-S8 (1997).
[6] M.M. Gottesman and I. Pastan, *J. Biol. Chem.* **263**, 12153-12166 (1988).
[7] S.V. Ambudkar, S. Dey, C.A. Hrycyna, M. Ramachandra, I. Pastan and M.M. Gottesman, *Annu. Rev. Pharmacol. Toxicol.*, **39**, 361-398 (1999).
[8] A.H., Schinkel, J.J. Smit, O. van Tellingen, *et al.*, *Cell*, 77, 491-502 (1994).
[9] S.G. Carter and D.W. Karl, *J. Biochem. Biophys. Methods*, 7, 7-13 (1982).
[10] B. Sarkadi, E.M. Price, R.C. Boucher *et al.*, *J. Biol. Chem.*, **267**, 4854-4858 (1992).
[11] A. Seelig, R. Gottschich and R.M. Devant, *Proc. Natl. Acad. Sci. USA*, **91**, 68-72 (1994).
[12] H. Fischer, R. Gottschlich and A. Seelig, *J. Membrane Biol.*, **165**, 201-211 (1998).
[13] http://thomsonderwent.com/products/patentresarch/markushtopfrag/
[14] http://thomsonderwent.com/derwenthome/media/support/userguides/chemindguide.pdf
[15] A.E. Senior, M.K. Al-Shawi and I.L. Urbatsch, *FEBS Lett.*, **377**, 285-289 (1995).
[16] Z.E. Sauna and S.V. Ambudkar, *Proc. Natl. Acad. Sci. USA*, **97**, 2515-2520 (2000).
[17] A. Garrigues, J. Nugier, S. Orlowski and E. Ezan, *Anal. Biochem.*, **305**, 106-114 (2002).
[18] U. Norinder, T. Österberg, P. Artursson, *Pharm. Res.*,, **14**, 1786-1791 (1997).
[19] T. Ishikawa, S. Kasamtsu, Y. Hagiwara, H. Mitomo, R. Kato and Y. Sumino, *Drug Metabol. Pharamcokin.*, **18**, 194-202 (2003).
[20] M.J. Rosen, Surfactants and Interfacial Phenomena, John Wiley & Sons, New York (1989).
[21] A. Seelig and E. Landwojtowicz, *Eur. J. Pharm. Sci.*, **12**, 31-40 (2000).
[22] G. Klopman, L.M. Shi and A. Ramu, *Mol. Pharmacol.*, **52**, 323-334 (1997).
[23] D. Schmid, G. Ecker, S. Kopp, M. Hitzler and P. Chiba, *Biochem. Pharm.*, **58**, 1447-1456 (1999).
[24] S. Etkins, R. B. Kim, B.F. Leake, A.H. Danzig, et al., *Mol. Pharmacol.*, **61**, 964-973 (2002)
[25] S. Etkins, R. B. Kim, B.F. Leake, A.H. Danzig, et al., *Mol. Pharmacol.*, **61**, 974-981 (2002)
[26] T.R. Stouch and O. Gudmundsson, *Adv. Drug. Delivery Rev.*, **54**, 315-328 (2002).
[27] T. Österberg, U. Norinder, *Eur. J. Pharm. Sci.*, **10**, 295-303 (2000).
[28] T. Ishikawa and W. Priebe, *Global Outsourcing Review*, **2**, 52-58 (2000).

European Journal of Neuroscience, Vol. 17, pp. 2249–2255, 2003

Role of heme oxygenase-1 protein in the neuroprotective effects of cyclopentenone prostaglandin derivatives under oxidative stress

Takumi Satoh,[1] Megumi Baba,[1] Daisaku Nakatsuka,[2] Yasuyuki Ishikawa,[3] Hiroyuki Aburatani,[4] Kyoji Furuta,[5] Toshihisa Ishikawa,[6] Hiroshi Hatanaka,[7] Masaaki Suzuki[5] and Yasuyoshi Watanabe[2]
[1]Department of Welfare Engineering, Faculty of Engineering, Iwate University, Morioka, Iwate 020–8551, Japan
[2]Department of Physiology, Osaka City University, Graduate School of Medicine, Osaka, Japan
[3]Division of Structural Cell Biology, Nara Institute of Science and Technology, Ikoma, Nara, Japan
[4]Department of Genomic Science, Research Center for Advanced Science and Technology, The University of Tokyo, Tokyo, Japan
[5]Regeneration and Advanced Medical Science, Graduate School of Medicine, Gifu University, Gifu, Japan
[6]Department of Biomolecular Engineering, Tokyo Institute of Technology, Midori-ku, Yokohama, Japan
[7]Division of Protein Biosynthesis, Institute for Protein Research, Osaka University, Suita, Osaka, Japan

Keywords: bilirubin, cortical neurons, cyclopentenone prostaglandin, heme oxygenase-1, HT22 cells, mice, NEPP

Abstract

Previously we found that some cyclopenteone prostaglandin derivatives (PGs), referred to as neurite outgrowth-promoting PGs (NEPPs), have dual biological activities of promoting neurite outgrowth and preventing neuronal death [Satoh *et al.* (2000) *J. Neurochem.*, **75**, 1092-1102; Satoh *et al.* (2001) *J. Neurochem.*, **77**, 50-62; Satoh *et al.* (2002) In Kikuchi, H. (ed.), *Strategenic Medical Science Against Brain Attack*. Springer-Verlag, Tokyo, pp. 78-93]. To investigate possible cellular mechanisms of the neuroprotective effects, we performed oligo hybridization-based DNA array analysis with mRNA isolated from HT22, a cell line that originated from a mouse hippocampal neuron. Several transcripts up-regulated by NEPP11 were identified. Because heme oxygenase 1 (HO-1) mRNA was the most prominently induced and was earlier reported to protect neuronal and non-neuronal cells against oxidative stress, we focused on it as a possible candidate responsible for the neuroprotective effects. We found NEPP11 to induce HO-1 protein (32 kDa) in HT22 cells in both the presence and the absence of glutamate, whereas non-neuroprotective prostaglandins (PGs) Δ^{12}-PGJ_2 or PGA_2 did not. Overexpression of HO-1-green fluorescence protein (GFP) fusion protein significantly protected HT22 cells against oxidative glutamate toxicity, whereas that of GFP alone did not. Furthermore, biliverdin and bilirubin, products of HO-1 enzymatic activity on heme, protected HT22 cells from oxidative glutamate toxicity. These results, together with our previous results, suggest that NEPP11 activates the expression of HO-1 and that HO-1 produces biliverdin and bilirubin, which result in the inhibition of neuronal death induced by oxidative stress. NEPP11 is the first molecular probe reported to have a neuroprotective action through induction of HO-1 in neuronal cells.

Introduction

Neurotrophins play an essential role in the maintenance of populations of neuronal cells from development through adulthood (Barde, 1998) and thus administration of neurotrophins may be an effective treatment for disorders of neurons (McMahon & Priestly, 1995). However, being proteins, neurotrophins are not ideal drug candidates owing to the low permeability of the blood–brain barrier to them. Therefore, much effort has been made in the search for non-peptidyl low-molecular-weight compounds (Saragovi & Gehring, 2000). Recently, we accumulated several lines of evidence showing that neurite outgrowth-promoting prostaglandins 11 (NEPP11) has neurotrophin-like, Trk-independent actions on central nervous system (CNS) neurons (Furuta *et al.*, 2000; T. Satoh *et al.*, 2000a, 2001). NEPP11 (a Δ^7-PG A_1 methyl ester derivative) was originally designed on the basis of the chemical structure of Δ^{12}-PGJ_2 (Fukushima, 1992; Suzuki *et al.*, 1997, 1998; Furuta *et al.*, 2000). NEPP11 is a novel type of neuroprotective compound characterized by its dual biological activities of promoting neurite outgrowth and preventing neuronal death (T. Satoh *et al.*, 2000a, b, 2001). Generally, the cyclopentenone-structured PGAs and PGJs exhibit antitumour activities both *in vivo* and *in vitro* (Honn *et al.*, 1981; Fukushima, 1992; Suzuki *et al.*, 1997, 1998). They accumulate in the nuclear fraction, where they bind to nuclear proteins (Narumiya *et al.*, 1987; Parker, 1995) and thereby modulate the expression of various genes (Holbrook *et al.*, 1992; Gorospe *et al.*, 1996; Ishikawa *et al.*, 1998; Tanikawa *et al.*, 1998). Transcriptional activation is required for the biological actions by the cyclopentenone-structured PGs (Fukushima, 1992). Thus, identification of the gene(s) responsible for their biological effects is critical to understand their intracellular mechanisms. Previous results suggest that induction of immunoglobulin heavy chain binding protein/glucose-regulated protein 78 plays a role in the promotion of neurite outgrowth by NEPPs (T. Satoh *et al.*, 2000a). During the comparison of biological activities among various PG derivatives, we noted that the intracellular mechanism involved in the neuroprotection was different from that involved in the promotion of neurite outgrowth (T. Satoh *et al.*, 2001).

Correspondence: Dr T. Satoh, as above.
E-mail: tsatoh@iwate-u.ac.jp

Received 18 December 2002, revised 31 March 2003, accepted 4 April 2003

doi:10.1046/j.1460-9568.2003.02688.x

In the present study, a DNA microarray analysis was performed to identify the gene responsible for the neuroprotective effect mediated by NEPP11. We found that the induction of heme oxygenase 1 (HO-1) protein plays a role in this neuroprotection. Finally, we propose that the differential regulations of HO-1/HO-2 activities comprise a transient- and sustained-phase cellular defence mechanism and co-operatively contribute to the maintenance of neuronal survival under oxidative conditions.

Materials and methods

Materials

PGA_2, Δ^{12}-PGJ_2 (Cayman Chemical, Ann Arbor, MI, USA), 3-(4,5-dimethylthiazol-2-yl)-2,5-diphenyl tetrazolium bromide (MTT; Research Organics, Cleveland, OH, USA), polyclonal antibody against rat HO-1 (SPA895, Stressgen, Victoria, Canada), biotinylated anti-rabbit IgG secondary antibody (Vector Laboratories, Burlingame, CA, USA), Cy™3 (Cy3)-conjugated streptavidin (Jackson Immuno Research Laboratories, West Grove, PA, USA), peroxidase-conjugated anti-rabbit IgG antibody (Biorad, Hercules, CA, USA), biliverdin, bilirubin and Hoechst 33,258 (Sigma, St. Louis, MO, USA) were used in this study. NEPPs were synthesized as reported previously (Furuta *et al.*, 2000).

HT22 cell culture

HT22 cells were cultured as described (T. Satoh *et al.*, 2000c). To evaluate cell survival of HT22 cells, we performed MTT assay according to a modification (Kubo *et al.*, 1995) of the original procedure (Mosmann, 1983).

RT-PCR analysis

For reverse transcription-polymerase chain reaction (RT-PCR) analysis of HO-1 mRNA, total RNA of HT22 cells was obtained at 0.5, 1.0, 2.0, 5.0 and 8.0 h after glutamate treatment by use of TRIZOL Reagent (Invitrogen Corp., Carlsbad, CA, USA). Total RNA 1 μg was exposed to MMLV reverse transcriptase (50 U) in the presence of RNasin (20 U), random hexamers (2.5 μM), dNTPs and the supplied reverse transcription buffer. The reaction (20 μL) was allowed to continue for 15 min at 42 °C. A 10-μL aliquot of this mixture was then subjected to PCR conducted with HO-1 (5′-ACT TTC AGA AGG GTC AGG TGT CC-3′ and 5′-TTG AGC AGG AAG GCG GTC TTA G-3′) or GAPDH (5′-ATG CCA GTG GC TTC CCG TTC AGC-3′ and 5′-ACC CCT TCA TTG ACC TCA ACT-3′) primers (5 μM each). At the completion of PCR, 10 μL of PCR products was mixed with 2 μL of loading buffer and electrophoresed in 1.5% agarose gel in the presence of 0.5 μg/mL of ethidium bromide. The amplified DNA fragments (523 and 504 bp for HO-1 and GAPDH, respectively) were visualized with a UV transilluminator.

DNA microarray analysis

Total RNA was obtained after a 6-h treatment of HT22 cells with glutamate or vehicle in the presence or absence of NEPP11 (1 μM) and subjected to DNA microarray analysis as described previously (Ishii *et al.*, 2000) by use of a DNA microarray plate (Genechip, Affymetrix, Santa Clara, CA, USA).

Western blot analysis

HT22 cells were lysed in cell lysis buffer after 24 h of glutamate treatment, as described previously (T. Satoh *et al.*, 2000c). The protein signals were detected with anti-rat HO-1 polyclonal antibody and enhanced by chemiluminesence (ECL™ Western blotting; Amersham Pharmacia Biotech., Buckinghamshire, UK).

Immunofluorescence analysis of HO-1

HT22 cells were fixed after 24 h of incubation with or without NEPP11 (1 μM). The signals originated from polyclonal antibody against rat HO-1 were enhanced by biotinylated anti-rabbit IgG secondary antibody followed by detection with Cy™3 (Cy3)-conjugated streptavidin as described previously (T. Satoh *et al.*, 2000a).

DNA construction and transfection

PCR was performed using rat HO-1 primers (5′-CTC AGA TCT ATG GAG CGC CCA CAG C-3′ and 5′-TCG AAG CTT CAT GGC ATA AAT TCC CAC TG-3′) and pCRHO-1 as a templete (Shibahara *et al.*, 1985), and then the PCR product was digested with *Bgl*II and *Hin*dIII and cloned in pEGFPN1 and pEGFPC1 (Clontech Laboratories Inc., Palo Alto, CA, USA). These resulting vectors, pHON1 and pHOC1, can express rat HO-1 protein fused in-frame with the N- and C-terminal portion of EGFP, respectively. DNA transfection was performed by a particle bombardment method using the PDS-1000He particle delivery system (Bio-Rad) as described previously (H. Satoh *et al.*, 2000) according to the manufacturer's instructions. Recently this method was reported to allow highly efficent DNA transfection of primary neurons (McAllister, 2000).

Results

NEPP11 had a potent protective effect on HT22 cells (Satoh *et al.*, 2001). A high concentration of glutamate in the culture medium induced neuronal death through oxidative stress 10 h after the exposure of glutamate as described previously (Schubert *et al.*, 1992; Davis & Maher, 1994; Tan *et al.*, 1998). The presence of NEPP11 (1.0 μM) almost completely protected HT22 cells against this toxicity (Satoh *et al.*, 2001).

To identify the gene responsible for the neuroprotective effect of NEPP11, we performed a DNA microarray analysis. Total RNA was isolated from control HT22 cells or the cells treated with NEPP11 (1.0 μM) for 6 h in the presence or the absence of glutamate (5 mM) and was subjected to reverse transcription and oligo hybridization-based DNA array analysis. Three genes showed significantly increased expression (sort score >1.5) in response to NEPP11 both in the presence and in the absence of glutamate. The sort score is used in DNA microarray analysis as a parameter to indicate data reliance of gene induction. These three genes encode stress proteins, HO-1, α-B-crystallin and tissue inhibitor of metalloproteinase-3 (TIMP-3). The fold increase of induction/sort score of HO-1, α-B-crystallin and TIMP3 was 4.1/2.65, 4.7/3.16 and 4.6/2.65, respectively; and in the presence of glutamate, 5.1/4.22, 3.3/1.51 and 3.9/1.9, respectively.

In this study, although the expression of α-B-crystallin and TIMP-3 were elevated by NEPP11, we focused on HO-1 for the following reasons: (1) cerebellar granule neurons from HO-1-transgenic mice are resistant to oxidative stress (Chen *et al.*, 2000), (2) gene transfer of α-B-crystallin did not protect fibroblasts from oxidative stress (Mehlen *et al.*, 1996) and (3) gene transfer of TIMP-3 enhanced cell death (Bian *et al.*, 1996). At first, the data from the DNA microarray analysis were confirmed by a RT-PCR experiment (Fig. 1A). Total RNA was extracted at various times after the addition of NEPP11 and subjected to reverse transcription by use of random primers and to PCR with primers for HO-1 and GAPDH. Although the levels of GAPDH mRNA was constant during the experiment, HO-1 mRNA was present at a very low level in control cells and increased between 0.5 and 2.0 h after the addition of NEPP11, suggesting that HO-1 mRNA was up-regulated by NEPP11. Next, using Western blotting, we examined the induction of HO-1 protein by various cyclopentenone PGs (Fig. 1B). Neuroprotective NEPP6 and NEPP11 increased the expression of

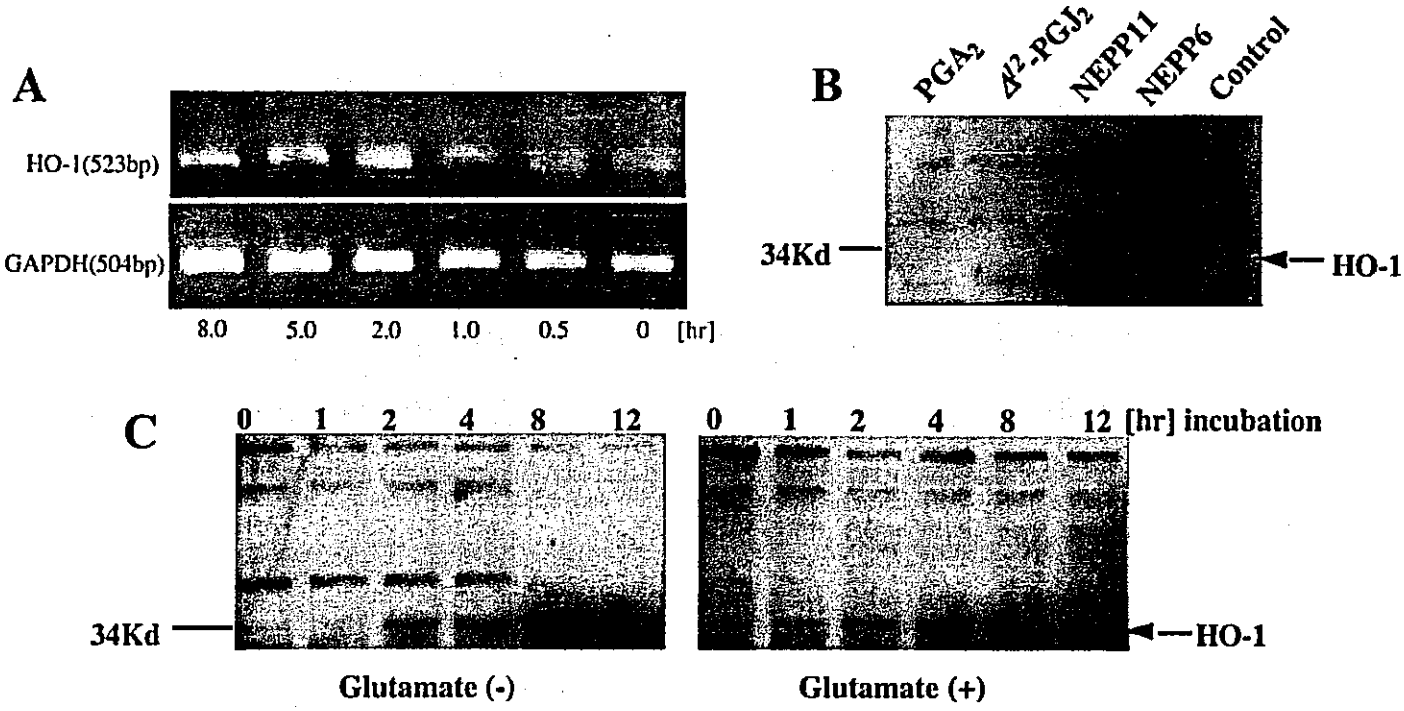

FIG. 1. (A) Time-dependent expression of HO-1 mRNA induced by NEPP11. HT22 cells were incubated for 0, 0.5, 1.0, 2.0, 5.0 or 8.0 h with NEPP11, and then total RNA was extracted and subjected to reverse transcription and to PCR with HO-1 or GAPDH primers. (B) Induction of HO-1 protein (32 kDa) by 1 μM NEPP6, 1 μM NEPP11, 2 μM PGA_2 or 2 μM Δ^{12}-PGJ_2. HT22 cells were incubated with various cyclopentenone PGs for 24 h, and then their lysates were subjected to Western blotting. (C) Time-dependent induction of HO-1 protein by 1 μM NEPP11. HT22 cells were cultured for various periods of time with 1 μM NEPP11 in the presence (right) or absence (left) of glutamate (5 mM), and then their lysates were prepared and subjected to Western blotting.

HO-1. In contrast, non-neuroprotective Δ^{12}-PGJ_2 and PGA_2 did not induce the protein. Time-dependent induction of HO-1 protein by 1 μM NEPP11 was examined in both the presence and the absence of 5 mM glutamate (Fig. 1C). The level of HO-1 protein increased after 2 h of incubation and reached its maximum at 8 h (Fig. 1C, left). The presence of glutamate did not make much difference (Fig. 1C, right). The induction of HO-1 was also confirmed by immunofluorescence (Fig. 2A and B). In this experiment, the average fluorescence intensity (arbitrary unit) in each designated square was obtained to provide quantitative comparison between control and NEPP11-treated cells. The NEPP11-treatd cells had much higher intensity [177.6 ± 22.8, mean ± SD ($n = 10$)] than did the control cells [83.5 ± 5.6 ($n = 10$)], indicating that NEPP11 effectively induced HO-1 protein in HT22 cells.

To provide evidence for the neuroprotective effects of HO-1 protein, we performed a gene transfer experiment by use of particle bombardment (Fig. 3). HO-1 protein fused in-frame to the C-terminal portion of GFP, termed GFP–HO-1, or GFP protein alone, could be expressed under the regulation of the CMV promoter. The transfection efficiency was $28.3 \pm 7.3\%$ of all cells (mean ± SD, $n = 6$). The expression patterns of GFP and GFP–HO-1 were quite different (Fig. 3A and B). GFP was sparsely expressed throughout the cells (Fig. 3A); in contrast, GFP–HO-1 was expressed in a particle-like fashion mainly in the cytoplasm (Fig. 3B). This pattern was identical to that of HO-1 protein fused in-frame to the N-terminal portion of GFP (HO-1–GFP)-expressed cells (data not shown). The cells transfected with GFP alone shrank 24 h after the addition of glutamate (Fig. 3C), whereas those transfected with GFP–HO-1 did not shrink after the additon of glutamate (Fig. 3D). We did not utilize DNA staining with propidium iodide or Hochest 33,258 for detection of cell death because non-transfected DNA was tightly attached to the cell surface, which would interfere with the measurement. Thus, we assessed death by cell shrinkage (<20 μm), which occurrs in neuronal death. The presence of glutamate for 24 h increased the number of shrunken cells transfected with GFP [$87.5 \pm 14.4\%$ of transfected cells ($n = 4$)]. In contrast, the cells transfected with GFP–HO-1 were much less shrunken [$6.25\% \pm 3.5\%$ ($n = 4$)] in the presence of glutamate. Similar results were obtained with the use of HO-1–GFP. These results show that the cells survived effectively when HO-1 protein was induced.

Is the enzymatic activity of HO-1 required for the neuroprotective effects? As biliverdin and bilirubin are products of HO-1 catalysis, we examined their effects on HT22 cells (Fig. 4). Both biliverdin and bilirubin significantly protected HT22 cells against oxidative glutamate toxicity, suggesting that the enzymatic activity of HO-1 plays some role in the inhibition of death of HT22 cells.

Discussion

HO cleaves heme molecules at the α-meso carbon bridge and produces the open tetrapyrrole biliverdin. This enzyme family comprises three isozymes, HO-1, HO-2 and HO-3. HO-1 and HO-2 have a different gene expression pattern (Maines, 1997). In contrast to the constitutive isoform HO-2, HO-1 is the heat shock/stress-inducible cognate of the heat shock protein 32 and is induced by its substrate heme and numerous stress stimuli such as UV light, heavy metals, lipopolysaccharide and hyperoxia (Shibahara, 1994; Maines, 1997). In the brain, HO-2 protein is abundantly expressed in neuronal populations, whereas HO-1 is expressed to a far lower level, and its level is markedly increased in glial cells in response to oxidative stress (Ewing & Maines, 1991). The activity of HO-2 is regulated by phosphorylation, and that of HO-1 at the transcriptional level (Shibahara, 1994; Maines, 1997; Dore *et al.*, 1999). Dore *et al.* (1999) reported that HO-2